Experimental Validation of a Fuzzy Adaptive Voltage Controller for Three-Phase PWM Inverter of a Standalone DG Unit

Dong Quang Dang, Young-Sik Choi, Han Ho Choi, *Member, IEEE*, and Jin-Woo Jung, *Member, IEEE*

***Abstract*—This paper investigates a disturbance observer-based fuzzy adaptive voltage controller for three-phase pulse width modulation (PWM) inverter of a standalone distributed generation (DG) unit in the existence of system uncertainties. The proposed control law includes only a voltage control loop, which has advantages such as a simple control structure and a fast transient response due to the direct control of the output voltage. Next, a disturbance observer is presented to reduce the number of the sensors and improve the control performance. Besides, the proposed strategy is insensitive to any system uncertainties, because it does not require any accurate knowledge about system parameter and load current information. Experimental results on a prototype DG unit with a TMS320F28335 DSP are demonstrated to validate the superior performance of the proposed control scheme over the conventional proportional-derivative (PD) control method and feedback linearization control (FLC) method under sudden load disturbances, system uncertainties, and nonlinear load.**

***Index Terms*—Adaptive control, distributed generation (DG) unit, disturbance observer, fuzzy control, standalone, voltage control.**

I. Introduction

DISTRIBUTED generation (DG) units based on renewable energy sources have highly increased in recent years since the greenhouse gas emissions and dependence of fossil fuels can be significantly reduced in [1] and [2]. In practice, the DG units can operate in grid-connected applications [3]–[5], or standalone applications [6]–[8] to supply power to grid or local loads, respectively. In grid-connected applications, the DG units are used for not only supplying electric power to the grid but also increasing the reliability of the grid. Meanwhile, in standalone applications, the DG units are popularly used for remote areas isolated from the grid. Also, in case of grid faults, grid-connected DG units are switched to an islanded mode like a standalone application to continuously provide electricity to local loads. Generally, the DG units in standalone operation should be capable of feeding local loads with precise and stable voltage and frequency. In addition, depending on power demand, multiple DG units can be connected in parallel; however, this produces a load-sharing issue between these DG units. To solve the above points in standalone DG units, many control methods in [9]–[11] are based on the cascade control structure, i.e., active and reactive power controllers in the outer loop and load voltage and frequency controllers in the inner loop. Note that the power and frequency controls can be designed by using droop and phase-locked loop controllers, respectively, as in [9]–[11]. Meanwhile, in case of standalone applications, the inner voltage control loop of multiple DG units can be designed by the same method as that of a single DG unit or a single uninterruptible power supply (UPS). However, it is quite challenging to precisely and robustly control its voltage in the existence of sudden load disturbances, system parameter uncertainties, nonlinear load, etc., as in [12]–[26]. In particular, the nonlinear loads such as a diode rectifier can make the load voltage strongly distorted due to the nonlinearity of the line-current waveforms. Therefore, the advanced voltage control schemes are actually required, which can guarantee the robustness to system uncertainties and low total harmonic distortion (THD) performance.

To overcome the above difficulties, many control algorithms have been proposed for a single standalone DG unit or UPS [12]–[26]. In [12] and [13], a load current observer-based model predictive voltage controller is presented. Although a load current observer [12] is established to enhance the behaviors of the controller without increasing the number of current sensors, the THD is still high. Moreover, the observer gains in [12] are highly dependent on the accuracy of both filter capacitance and inductance. In [14] and [15], a repetitive control scheme for three-phase UPS inverters is investigated. This algorithm shows low THD under unbalanced load and nonlinear load, but the transient responses are quite slow. Two iterative learning control schemes that include a direct iterative learning control and a hybrid iterative learning control are described in [16]. These strategies can achieve a high performance; however, the design procedure is complicated. Feedback linearization control (FLC) technique [17] can obtain a fast dynamic response and low THD. However, this algorithm is highly dependent on the precise parameters of inductor-capacitor (LC) filter. In [18], the differential flatness technique-based control method using only one voltage control loop is robust to load disturbances and LC filter parameter variations. Nevertheless, this algorithm meets a high computational burden, and the transient

Manuscript received July 03, 2014; revised October 15, 2014, December 09, 2014, and February 27, 2015; accepted March 18, 2015. Date of publication March 25, 2015; date of current version June 02, 2015. This work was supported in part by the National Research Foundation of Korea (NRF) under Grant 2012R1A2A2A01045312 and Grant 2014R1A2A1A11049543 funded by the Korea government [Ministry of Science, Information and Communication Technology (ICT), and Future Planning (MISP)]. Paper no. TII-14-0602.

The authors are with the Division of Electronics and Electrical Engineering, Dongguk University, Seoul 100-715, Korea (e-mail: jinwjung@dongguk.edu).

Color versions of one or more of the figures in this paper are available online at http://ieeexplore.ieee.org.

Digital Object Identifier 10.1109/TII.2015.2416981

response appears to be quite sluggish. Sliding mode control schemes studied in [19] and [20] are quite insensitive to system uncertainties. In [19], the discrete-time sliding mode control scheme is designed as the cascade structure with the current predictor in an outer loop and the current controller in an inner loop; nonetheless, the THD of the load voltage is quite high in case of nonlinear load. In [20], although a good performance can be attained under some severe load conditions, the voltage controllers are only applied for single-phase inverters. In [21], the authors introduce a robust servomechanism controller for three-phase inverter of a standalone DG unit. Even, if this scheme shows the possibility to attain a fast dynamic response and low steady-state error, it requires exact parameter values of resistor-inductor-capacitor (RLC) load. In [22], the three-phase four-wire inverter control technique of a single DG unit contains a discrete-time sliding mode current control in an inner loop and a robust servomechanism controlled voltage in an outer loop. In that paper, the simulation and experimental results indicate a good performance under unbalanced load, step load change, and nonlinear load, but the space vector pulse width modulation (PWM) technique needs be complexly modified. In [23] and [24], the authors present the dissipativity-based adaptive control, which can accurately follow the voltage reference of three-phase UPS system in the existence of system parameter uncertainties. However, these control algorithms look complicated since many parameters are adapted. In [25], a load current observer-based adaptive control scheme of a single standalone DG unit is improved from the proportional-derivative (PD) control technique. This control algorithm can guarantee a good performance under several load conditions; however, both observer and controller need the precise value of the filter capacitance. Consequently, this observer-based adaptive control scheme may significantly degrade the voltage regulation as the filter capacitance varies. Moreover, there is lack of the design procedure to tune the gains of the feedback control term. In [26], another adaptive control method is also applied for a single standalone DG unit. This control algorithm based on Riccati-like inequality is quite complicated, and its cost effectiveness is not achieved because it needs load current sensors instead of a load current observer.

This paper presents a fuzzy adaptive voltage control strategy for a single standalone DG unit. To deal with system uncertainties, a fuzzy adaptive compensating control term is proposed. Because the proposed controller consists of only a voltage control loop, in which the output voltage is directly regulated, it possesses a simple control structure and can obtain fast transient responses. To enhance the reliability and control performance, a disturbance observer is designed to estimate all the disturbances such as load disturbances, system parameters uncertainties, and noises. Also, the proposed controller as well as the proposed observer is robust to system uncertainties as they do not require any precise knowledge of system parameters and load currents. Experimental results, with comparison to the conventional PD control method and the feedback linearization control (FLC) method, are given to confirm the validity of the proposed observer-based control scheme under sudden load disturbances, system parameter uncertainties, and nonlinear load.

The outline of this paper is as follows. A fuzzy adaptive voltage controller based on Lyapunov function is analyzed in Section II, and an adaptive disturbance observer is described in Section III. In Section IV, experimental results are presented, and conclusion is summarized in Section V.

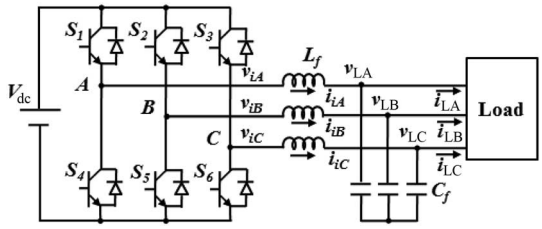

Fig. 1. Circuit configuration of a three-phase PWM inverter with an LC output filter for a standalone DG unit.

II. Design of Fuzzy Adaptive Voltage Controller

A. Mathematical Model of a Single Standalone DG Unit With System Uncertainties

Fig. 1 illustrates the circuit diagram of a three-phase PWM inverter with an LC output filter for a single standalone DG unit. As shown in Fig. 1, it is comprised of four parts: 1) a dc-link voltage ($V_{\rm dc}$) from renewable energy sources; 2) a three-phase PWM inverter (S_1 to S_6); 3) an LC output filter (L_f and C_f); and 4) a three-phase load. As shown in Fig. 1, the renewable energy sources and ac–dc or dc–dc power converter are modeled as a stiff dc voltage source ($V_{\rm dc}$) since most DG units includes the energy storage devices [27]–[29] (e.g., batteries, and ultra-capacitors) with the bidirectional dc–dc converter, or the energy dissipation devices [30] (e.g., dc-chopper circuit with a resistor) in order to absorb or dissipate the excess power overflowed from the DG unit or the load and then properly regulate the dc-link voltage level overcharged within an acceptable voltage range. In the synchronously rotating dq reference frame, a single standalone DG unit with an LC filter can be modeled by the following dynamic equations including system uncertainties [25]

$$\begin{aligned} \dot{v}_{Ldq} &= M v_{Ldq} + \frac{1}{C_f} i_{idq} - \frac{1}{C_f} d_{1dq} \\ \dot{i}_{idq} &= M i_{idq} - \frac{1}{L_f} v_{Ldq} + \frac{1}{L_f} v_{idq} - \frac{1}{L_f} d_{2dq} \end{aligned} \tag{1}$$

where

$$\begin{aligned} M &= \begin{bmatrix} 0 & \omega \\ -\omega & 0 \end{bmatrix}, \begin{bmatrix} d_{1dq} \\ d_{2dq} \end{bmatrix} \\ &= \begin{bmatrix} i_{Ldq} + \Delta C_f \dot{v}_{Ldq} - \Delta C_f M v_{Ldq} \\ \Delta L_f \dot{i}_{idq} - \Delta L_f M i_{idq} \end{bmatrix} \end{aligned}$$

$v_{idq} = [v_{id}\ v_{iq}]^T$ inverter $d-q$ axis voltage;
$i_{idq} = [i_{id} i_{iq}]^T$ inverter $d-q$ axis current;
$v_{Ldq} = [v_{Ld}\ v_{Lq}]^T$ load $d-q$ axis voltage;
$i_{Ldq} = [i_{Ld} i_{Lq}]^T$ load $d-q$ axis current;
$C_f,\ L_f$ nominal values of output filter capacitance and inductance, respectively;
$\Delta C_f,\ \Delta L_f$ uncertainties of output filter capacitance and inductance, respectively;

ω	angular frequency ($\omega = 2\pi \cdot f$);
f	fundamental frequency of voltage or current;
d_{1dq}, d_{2dq}	disturbance representing load disturbance (i_{Ldq}) and parameter uncertainties ($\Delta C_f,\ \Delta L_f$).

Compared to the sampling time [12], the disturbances vary slowly; thus, the model (1) can be transformed into

$$\ddot{v}_{Ldq} = \frac{1}{L_f C_f} v_{idq} - f_{dq} \tag{2}$$

where f_{dq} is the function of unknown system uncertainties and expressed as follows:

$$f_{dq} = -M\dot{v}_{Ldq} + \frac{1}{L_f C_f} v_{Ldq} - \frac{1}{C_f} M i_{idq} + \frac{1}{L_f C_f} d_{2dq}.$$

It is observed from (2) that the control objective is to regulate that the load voltage v_{Ldq} can accurately track the reference $v_{Ldq\_\mathrm{ref}} = [v_{\mathrm{dref}} v_{\mathrm{qref}}]^T$ using the control input v_{idq}. Let us define the fictitious control input (V_{idq}) and the load voltage error ($\bar{v}_{Ldq}$) as follows:

$$v_{idq} = L_f C_f V_{idq}, \quad \bar{v}_{Ldq} = v_{Ldq} - v_{Ldq\_\mathrm{ref}}. \tag{3}$$

Assume that the reference load voltage v_{Ldq_ref} and its first-order time derivative are kept constant during all sampling periods [25]. Thus, it is observed from (3) that the first- and second-order time derivatives of the load voltage and the load voltage error are the same. Therefore, the model (2) can be represented as

$$\ddot{\bar{v}}_{Ldq} = V_{idq} - f_{dq}. \tag{4}$$

B. Proposed Fuzzy Adaptive Voltage Controller Based on Lyapunov Function

The fictitious control input defined in (3) is separated into the following two control terms:

$$V_{idq} = u_{\mathrm{fb}} + u_{\mathrm{ff}}. \tag{5}$$

Note that the former term is the state feedback control term ($u_{\mathrm{fb}} = [u_{\mathrm{fb1}} u_{\mathrm{fb2}}]^T$) that stabilizes the system error dynamics, whereas the latter term is the compensating control term ($u_{\mathrm{ff}} = [u_{\mathrm{ff1}} u_{\mathrm{ff2}}]^T$), which deals with system uncertainties.

First, the state feedback control term is adopted as

$$u_{\mathrm{fb}} = -((\alpha + \beta)\dot{\bar{v}}_{Ldq} + \alpha\beta\bar{v}_{Ldq}) \tag{6}$$

where α and $\beta > 0$.

Then, let us define the following input variable:

$$\sigma = \begin{bmatrix} \sigma_1 & \sigma_2 \end{bmatrix}^T = \dot{\bar{v}}_{Ldq} + \beta\bar{v}_{Ldq}. \tag{7}$$

Next, a fuzzy control is applied to design the compensating control term that deals with the uncertain term f_{dq}. It should be noted that the fuzzy approach has been shown to be very effective for taking account of system uncertainties without accurate mathematical models in the literature such as [31]. Based on a standard fuzzy inference method as shown in [31], the ith rule of the compensating control term is represented by a set of fuzzy rules of the following form:

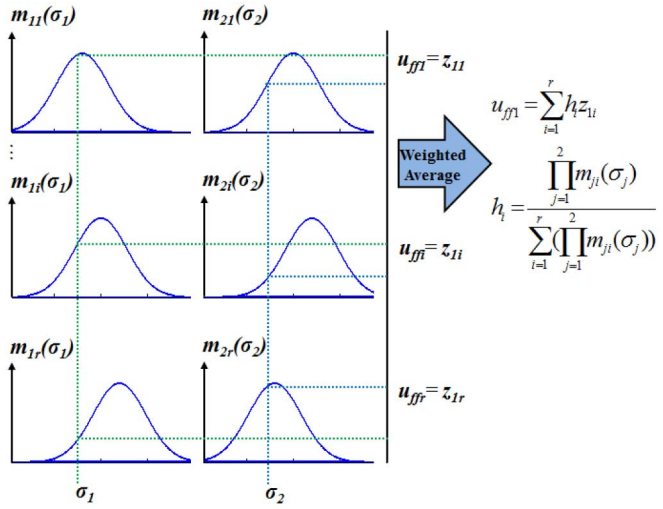

Fig. 2. Detailed illustration of the fuzzy inference method based on a weighted average defuzzifier to calculate the compensating control term u_{ff1}.

Rule i for u_{ff1}: If σ_1 is M_{1i} and σ_2 is M_{2i}, then $u_{\mathrm{ff1}} = z_{1i}$

Rule i for u_{ff2}: If σ_1 is M_{1i} and σ_2 is M_{2i}, then $u_{\mathrm{ff2}} = z_{2i}$

where $M_{ji} (i = 1, 2, \ldots, r, \quad j = 1, 2)$ are the fuzzy sets, r is the number of fuzzy rules, and z_{1i} and z_{2i} are the adjustable parameters. Then, the standard fuzzy inference method based on a weighted average defuzzifier is used to calculate the compensating control term (u_{ff}) as shown in Fig. 2

$$u_{\mathrm{ff}} = \begin{bmatrix} u_{\mathrm{ff1}} \\ u_{\mathrm{ff2}} \end{bmatrix} = \begin{bmatrix} \sum_{i=1}^{r} h_i z_{1i} \\ \sum_{i=1}^{r} h_i z_{2i} \end{bmatrix} = H\boldsymbol{Z} \tag{8}$$

where $\boldsymbol{Z} = [z_{11}, z_{12}, \ldots, z_{1r}, z_{21}, z_{22}, \ldots, z_{2r}]^T$

$$\mathrm{H} = \begin{bmatrix} h_1 & h_2 & \ldots & h_r & 0 & 0 & \ldots & 0 \\ 0 & 0 & \ldots & 0 & h_1 & h_2 & \ldots & h_r \end{bmatrix}$$

$$h_i = \frac{\prod_{j=1}^{2} m_{ji}(\sigma_j)}{\sum_{k=1}^{r} \left(\prod_{j=1}^{2} m_{jk}(\sigma_j) \right)}, \quad i = 1, 2, \ldots, r \tag{9}$$

h_i represents the normalized weight of ith fuzzy rule, which satisfies $h_i \geq 0$ and the sum of h_i is 1. Also, $m_{ji}(\sigma_j)$ is the membership function of input variables σ_j in fuzzy sets M_{ji} and is defined as

$$m_{ji}(\sigma_j) = \exp\left[-\frac{(\sigma_j - \varepsilon_{ji})^2}{(\delta_{ji})^2} \right] \tag{10}$$

where ε_{ji} and δ_{ji} denote the center and width values of the membership function m_{ji}, respectively.

Assume that the nonlinear uncertain term f_{dq} can be approximated by using the above fuzzy system and there exists a constant parameter vector $\boldsymbol{Z}^* \in R^{2r \times 1}$ such that $f_{dq} = H \times \boldsymbol{Z}^*$ as in [25] and [31]. Therefore, from (5), (6), and (8), the model (4) can be represented as

$$\ddot{\bar{v}}_{Ldq} = -((\alpha + \beta)\dot{\bar{v}}_{Ldq} + \alpha\beta\bar{v}_{Ldq}) + H\boldsymbol{Z} - H\boldsymbol{Z}^*. \tag{11}$$

As mentioned above, the compensating control term (u_{ff}) is aimed to deal with the system uncertainties (f_{dq}). Thus, the

adaptive law design for the parameter vector $\boldsymbol{Z}$ is required [31], and it can be derived from minimizing the following function:

$$E = 0.5\sigma^T\sigma. \tag{12}$$

Note that from (7) and (11), it is easy to obtain the following result:

$$\dot{\sigma} = -\alpha\sigma + H\boldsymbol{Z} - H\boldsymbol{Z}^*. \tag{13}$$

Based on the back-propagation rule, the vector $\boldsymbol{Z}$ is calculated by

$$\dot{\boldsymbol{Z}} = -\eta\frac{\partial E}{\partial Z} = -\eta\frac{\partial E}{\partial \sigma}\frac{\partial \sigma}{\partial Z} = -\eta H^T\sigma, \quad \eta > 0. \tag{14}$$

The following voltage control law enforces the voltage errors to converge to zero

$$V_{idq} = -((\alpha+\beta)\dot{\bar{v}}_{Ldq} + \alpha\beta\bar{v}_{Ldq}) + H\boldsymbol{Z}. \tag{15}$$

Let the Lyapunov function be chosen as

$$V = 0.5(\sigma^T\sigma + \bar{\boldsymbol{Z}}^T\eta^{-1}\bar{\boldsymbol{Z}}) \tag{16}$$

where $\bar{\boldsymbol{Z}} = \boldsymbol{Z} - \boldsymbol{Z}^*$. The time derivative of (16) is given by

$$\begin{aligned}\dot{V} &= \sigma^T\dot{\sigma} + \bar{\boldsymbol{Z}}^T\eta^{-1}\dot{\bar{\boldsymbol{Z}}} \\ &= \sigma^T(-\alpha\sigma + H\bar{\boldsymbol{Z}}) + \bar{\boldsymbol{Z}}^T\eta^{-1}\dot{\boldsymbol{Z}} \\ &= -\alpha\sigma^T\sigma + \sigma^T H\bar{\boldsymbol{Z}} - \bar{\boldsymbol{Z}}^T\eta^{-1}\eta H^T\sigma \\ &= -\alpha\sigma^T\sigma + \sigma^T H\bar{\boldsymbol{Z}} - \bar{\boldsymbol{Z}}^T H^T\sigma = -\alpha\sigma^T\sigma < 0.\end{aligned} \tag{17}$$

Then, by integrating both sides of (17), the following equation is derived

$$\alpha\int_0^\infty \sigma^T\sigma d\tau = V(0) - V(\infty) \le V(0) \le \infty. \tag{18}$$

which implies that $\sigma \in L_2 \cap L_\infty$ and $\boldsymbol{Z} \in L_\infty$.

From (7), the transfer function $G(\mathrm{s})$ from σ to $\bar{v}_{Ldq}$ is obtained by the following strictly positive function:

$$G(s) = \frac{1}{s+\beta}. \tag{19}$$

Finally, it is concluded from [32] that the voltage error $\bar{v}_{Ldq}$ converges exponentially to zero.

Note that the gains of the state feedback control term (like PD control method) can be easily designed using the pole placement method as indicated in [17]. In fact, by matching the second-order equation ($s^2 + (\alpha+\beta)s + \alpha\beta = 0$) with the desired characteristic polynomial $p(s) = (s-s_1)(s-s_2)$, where s_1 and s_2 are desired poles, the control gains can be selected as $\alpha = -s_1$ and $\beta = -s_2$. On the other hand, from (8) and (14), the gain of the compensating control term (η) can be easily tuned by the rules presented in [25]. Finally, the controller gains ($\alpha, \beta,$ and η) can be properly tuned by the following procedure.

1) Choose the gains α and β based on the desired characteristic polynomial $p(s)$.
2) Set η to quite small values and then increase η by a small amount.
3) If the transient and steady-state performances are satisfactory, then this process is completed. If not, go to Step 2).

III. Design of Disturbance Observer

The proposed control law (15) needs the information of the time derivative of the load voltage. In fact, this value can be directly calculated from the time derivative of the load voltage. However, this calculation strategy can be heavily affected by noises. Alternatively, as seen in the first equation of (1), the time derivative of the load voltage can be obtained if the disturbance d_{1dq} is known. Thus, in this section, a simple disturbance observer is proposed for estimating the disturbance d_{1dq}.

As indicated in [12], the disturbances vary slowly during the sampling time. Thus, from the model (1), the state-space model can be established in the following:

$$\dot{v}_{Ldq} = Mv_{Ldq} + \frac{1}{C_f}(i_{idq} - d_{1dq}), \quad \dot{d}_{1dq} = 0. \tag{20}$$

Then, the disturbance observer can be constructed as

$$\begin{aligned}\dot{\hat{v}}_{Ldq} &= Mv_{Ldq} - 2\lambda\bar{v}_o + \frac{1}{C_f}(i_{idq} - \hat{d}_{1dq}) \\ \dot{\hat{d}}_{1dq} &= \gamma\frac{1}{C_f}\bar{v}_o\end{aligned} \tag{21}$$

where $\bar{v}_o = \hat{v}_{Ldq} - v_{Ldq}$, and γ and λ are the observer gains. From (20) and (21), the error dynamics is given as follows:

$$\dot{\bar{v}}_o = -2\lambda\bar{v}_o - \frac{1}{C_f}\bar{d}_o, \quad \dot{\bar{d}}_o = \gamma\frac{1}{C_f}\bar{v}_o \tag{22}$$

where $\bar{d}_o = \hat{d}_{1dq} - d_{1dq}$.

Assume that the observer gains satisfy the conditions of $\lambda > 0$ and $\gamma = \lambda^2 C_f^2$, then the estimation error converges to zero.

From (22), the following dynamic equation can be obtained

$$\ddot{\bar{v}}_o + 2\lambda\dot{\bar{v}}_o + \gamma\frac{1}{{C_f}^2}\bar{v}_o = 0. \tag{23}$$

With $\gamma = \lambda^2 C_f^2$, the above dynamics can be reduced to

$$\ddot{\bar{v}}_o + 2\lambda\dot{\bar{v}}_o + \lambda^2\bar{v}_o = 0. \tag{24}$$

The roots of the second-order derivative equation (24) can be generally expressed as

$$\bar{v}_o(t) = (a_1 + a_2 t)e^{-\lambda t} \tag{25}$$

where a_1 and a_2 are constants. From (22) and (25), we also have

$$\bar{d}_o(t) = -C_f(a_1\lambda + a_2 + a_2\lambda t)e^{-\lambda t}. \tag{26}$$

With $\lambda > 0$, the results in (25) and (26) imply that the error dynamics converge to zero with a decay rate λ as time approaches infinity. Finally, the time derivative of the load voltage is calculated as follows:

$$\dot{v}_{Ldq} = Mv_{Ldq} + \frac{1}{C_f}(i_{idq} - \hat{d}_{1dq}). \tag{27}$$

As shown in (25) and (26), the error dynamics converge to zero with a decay rate λ. Therefore, to design the observer with a fast dynamic response, the observer gain λ is tuned to large values. Lastly, the observer gain λ can be systematically tuned as the following.

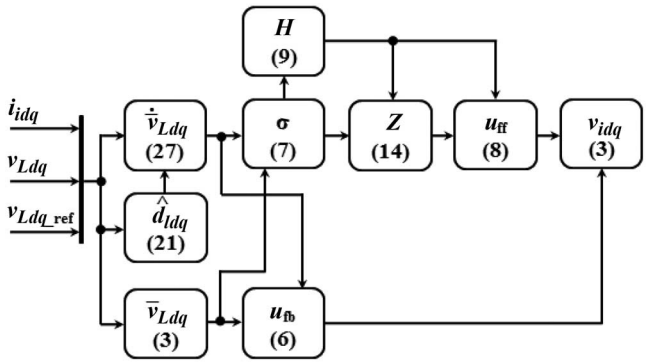

Fig. 3. Block diagram of the proposed observer-based fuzzy adaptive voltage control law.

TABLE I
SYSTEM AND CONTROL PARAMETERS

Items		Symbol	Value
System parameters			
DG unit rated power		P_{rated}	1 kVA
DC-link voltage		V_{dc}	295 V
LC output filter		C_f	6.67 μF
		L_f	10 mH
Desired load output voltage		$V_{L\text{-rms}}$	110 V
		f	60 Hz
Switching and sampling frequency		f_z	5 kHz
Linear load		R_l	36 Ω
Nonlinear load		R_n	65 Ω
		L_n	15 mH
		C_n	220 μF
Control parameters			
Controller gains	State feedback control term	α, β	$0.002/L_f/C_f$
	Compensating control term	η	0.3
Observer gains		λ	10 000
		γ	$\lambda^2 C_f^2$

1) Set λ to quite small values and then increase λ by a small amount.
2) If the observer performance is satisfied, then this process is completed. Else, return to Step 1).

From the proposed controller and observer, the proposed observer-based control law can be synthesized with the block diagram shown in Fig. 3. Finally, the design procedure can be summarized as follows.

1) Choose the observer gains λ and γ as explained above. Compute the estimated disturbance from (21). Then, referring to (27), calculate the time derivative of the load voltage.
2) Choose the control gains α and β based on the desired characteristic polynomial $p(s)$ as described in Section II. Design the state feedback control term from (6).
3) Choose the membership functions (10) for variables (σ_1 and σ_2). Next, construct the matrix H based on (9).
4) Choose the controller gain η as mentioned in Section II. Then, design the compensating control term from (7), (14), and (8).
5) Construct the control input from (3).

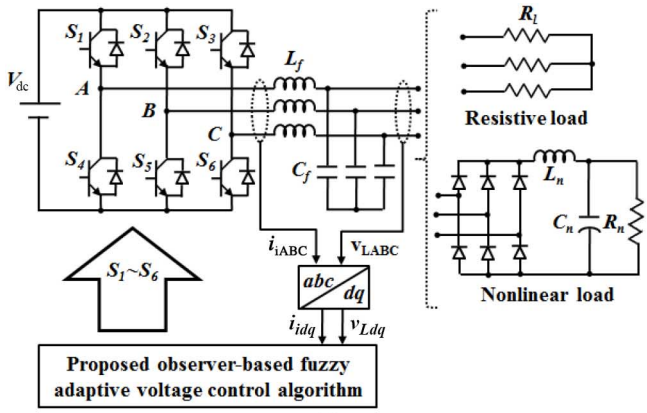

(a)

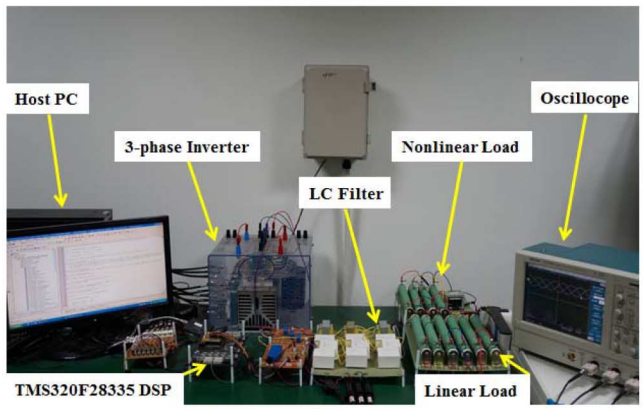

(b)

Fig. 4. Three-phase PWM inverter with an LC output filter for a single standalone DG unit. (a) Block diagram. (b) Experimental setup.

IV. EXPERIMENTAL RESULTS AND DISCUSSIONS

In this section, experiments are implemented on a prototype 1-kVA DG unit to justify the validity of the proposed control strategy. Table I indicates the system and control parameters. In Table I, the filter capacitance (C_f) and filter inductance (L_f) are designed as 6.67 μF and 10 mH, respectively, considering the filter performance, system cost, and power level. Also, the root mean square (rms) value ($V_{L\text{-rms}}$) and fundamental frequency (f) of the desired load voltage are set to 110 V and 60 Hz, respectively. It is noticed that the switching frequency (f_z) of the three-phase PWM inverter is selected as 5 kHz by taking into account a tradeoff between the control performance and the system efficiency. In this study, a space-vector PWM technique is utilized in order to generate symmetrical PWM pulses to six power switches of the three-phase inverter due to its key benefits that can provide the load with less harmonic voltages. Fig. 4(a) illustrates the block diagram of a three-phase PWM inverter with an LC output filter for a single standalone DG unit, whereas Fig. 4(b) shows the photograph of the experimental setup employed to carry out the proposed observer-based fuzzy adaptive voltage control law. As depicted in Fig. 4(b), the proposed control algorithm is implemented by a Texas Instruments TMS320F28335 DSP, which is extensively used for industrial control applications. This DSP has the following advantages: high-speed real-time signal processing with

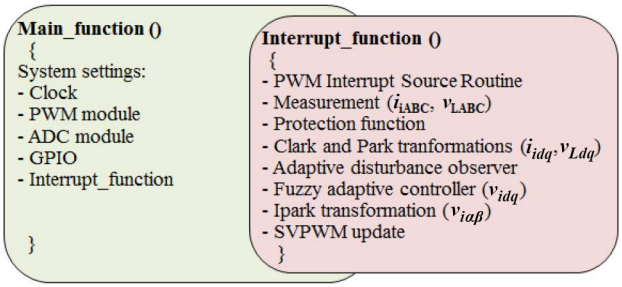

Fig. 5. DSP program layout of the proposed control algorithm in C-language.

a clock frequency of 150 MHz, and tightly integrated peripherals such as the 12-bit A/D converters with 2×8 input channels and the PWM modules with 6×2 output channels. In this paper, the 12-bit A/D converter is used to convert the inverter currents (i_{iABC}) and load output voltages (v_{LABC}) from the analog values to the digital values and then the sampled quantities are reflected in the proposed control algorithm at each PWM switching instant. Fig. 5 illustrates the DSP program layout of the proposed control algorithm in C-language. Note that the proposed observer-based control algorithm is executed in the interrupt function, which is called when the counter of the PWM modules operating in an up-down mode is reset. It means that the newly updated control inputs (v_{idq}) can be applied at each PWM switching instant.

As presented previously, the proposed voltage controller consists of two main control terms: 1) the state feedback control term (u_{fb}) (like the conventional PD control); and 2) the adaptive control term (u_{ff}). Therefore, to definitely validate the improvements of the proposed voltage control law against system uncertainties, the conventional PD control method is adopted because it has the control structure similar to the proposed control method. Also, for fair comparison, the gains (α, β) of the conventional PD controller are chosen with the same values as those of the feedback control term (u_{fb}) of the proposed voltage controller, i.e., the control input of the conventional voltage controller is determined as $v_{idq} = L_f C_f u_{\mathrm{fb}}$, where u_{fb} is the same as (6). Note that both the proposed and conventional voltage controllers need the information of the time derivative of the load voltage. Conventionally, this derivative term can be directly calculated from the load voltage. However, this direct method cannot accurately obtain the derivative term due to high frequency noises. Thus, as presented in (27), this derivative component is indirectly computed based on the proposed disturbance observer, which not only can precisely estimate its time derivative but also can avoid high frequency noise components due to the direct calculation method. Therefore, the proposed disturbance observer can enhance the control performance (i.e., low ripple or low THD). To demonstrate the advantage of the proposed observer, the derivative-based estimation of the load voltage is incorporated to the conventional PD voltage controller. Based on Sections II and III, the observer and controller gains of the proposed control method are selected as in Table I. In addition, the FLC method with only one control loop [17], which has been widely used for the voltage control of a single standalone DG unit in recent years, is investigated in order to clearly prove the better performance of the proposed observer-based control law.

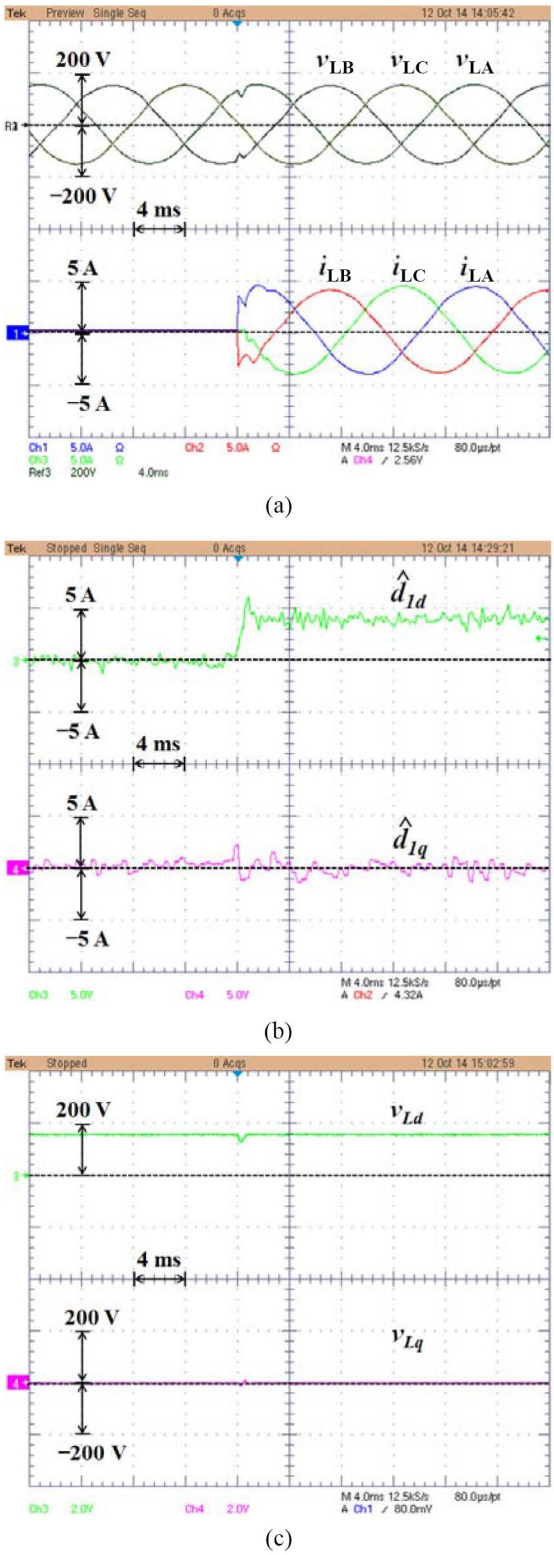

Fig. 6. Experimental results of the proposed control scheme under sudden load disturbance with system uncertainties ($\Delta L_f = +0.6L_f, \Delta C_f = +0.6C_f$). (a) Load voltages ($v_{\mathrm{LA}}, v_{\mathrm{LB}}, v_{\mathrm{LC}}$) and load currents ($i_{\mathrm{LA}}, i_{\mathrm{LB}}, i_{\mathrm{LC}}$). (b) Estimated disturbance ($\hat{d}_{1d}$, $\hat{d}_{1q}$). (c) Load $d-q$ axis voltages ($v_{\mathrm{Ld}}, v_{\mathrm{Lq}}$).

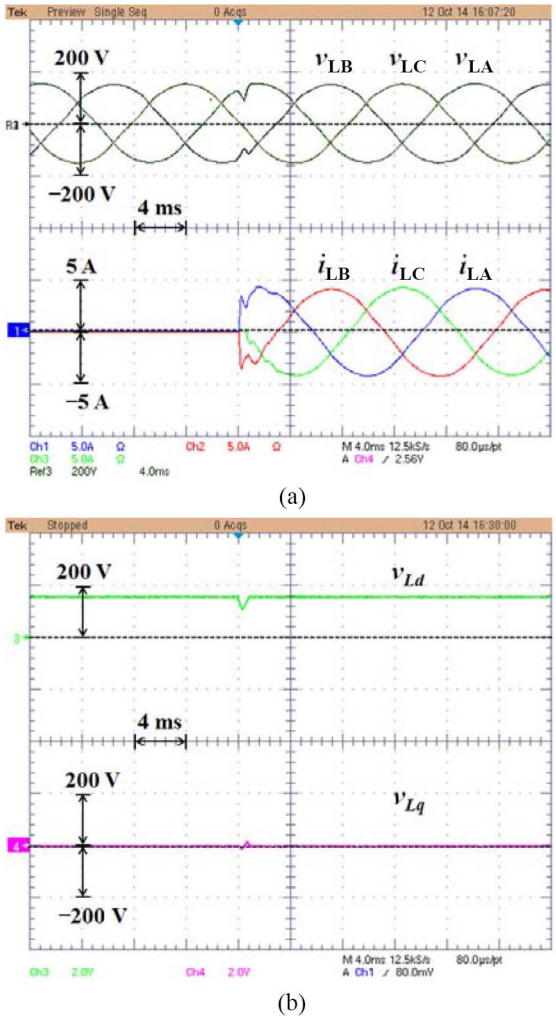

Fig. 7. Experimental results of the conventional PD control scheme under sudden load disturbance with system uncertainties ($\Delta L_f = +0.6L_f$, $\Delta C_f = +0.6C_f$). (a) Load voltages ($v_{\rm LA}, v_{\rm LB}, v_{\rm LC}$) and load currents ($i_{\rm LA}, i_{\rm LB}, i_{\rm LC}$). (b) Load $d-q$ axis voltages ($v_{\rm Ld}, v_{\rm Lq}$).

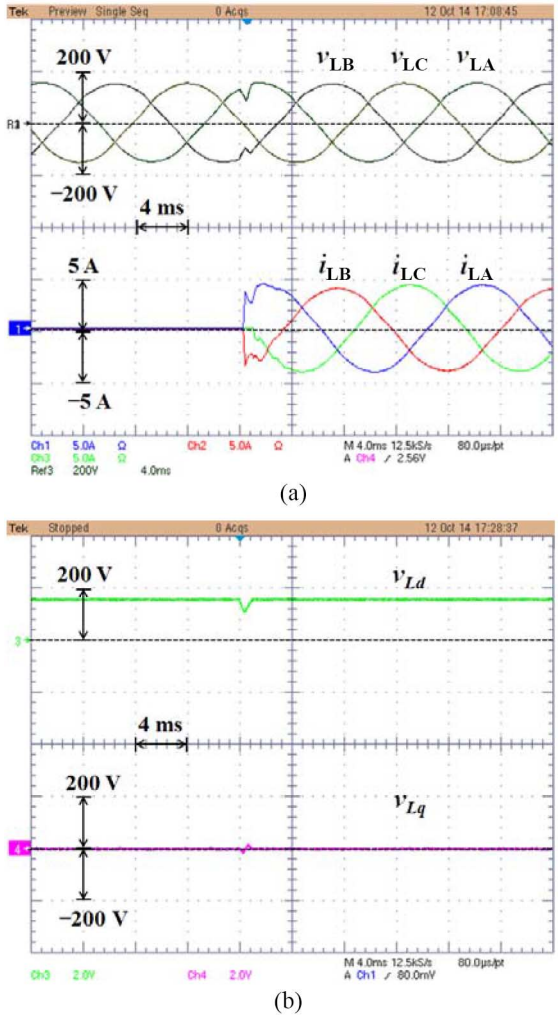

Fig. 8. Experimental results of the FLC scheme under sudden load disturbance with system uncertainties ($\Delta L_f = +0.6L_f, \Delta C_f = +0.6C_f$). (a) Load voltages ($v_{\rm LA}, v_{\rm LB}, v_{\rm LC}$) and load currents ($i_{\rm LA}, i_{\rm LB}, i_{\rm LC}$). (b) Load $d-q$ axis voltages ($v_{\rm Ld}, v_{\rm Lq}$).

It is noted that the control performance can get better if the numbers of the fuzzy rules and membership functions increase. However, it results in a complex control structure. Therefore, there is always a tradeoff between an acceptable control performance and a simple control structure. In this paper, only four membership functions of two fuzzy sets for two input variables (σ_1 and σ_2) are taken for use in an experimental study, which can guarantee both a satisfactory performance and a simple control structure as follows:

$$m_{P1}(\sigma_1) = e^{-(\sigma_1-10)^2/(20)^2},\ m_{N1}(\sigma_1) = e^{-(\sigma_1+10)^2/(20)^2}$$
$$m_{P2}(\sigma_2) = e^{-(\sigma_2-10)^2/(20)^2},\ m_{N2}(\sigma_2) = e^{-(\sigma_2+10)^2/(20)^2}.$$

Also, the above membership functions are based on the Gaussian function that can cover a large range of input variables and denote the relationship between input and output variables in a simple way. The center and width values of the membership functions are appropriately designed to guarantee that the fuzzy sets for the input variables σ_1 and σ_2 cover $\sigma_1 = 0$ and $\sigma_2 = 0$, respectively, as explained in [33] and [34]. Then, the number of fuzzy rules can be constructed as $r = 2 \times 2 = 4$, and these fuzzy rules are used for $u_{\rm ff1}$ and $u_{\rm ff2}$ as the following:

Rule 1: If σ_1 is P_1 and σ_2 is P_2, then $u_{\rm ff1} = z_{11}(u_{\rm ff2} = z_{21})$;
Rule 2: If σ_1 is P_1 and σ_2 is N_2, then $u_{\rm ff1} = z_{12}(u_{\rm ff2} = z_{22})$;
Rule 3: If σ_1 is N_1 and σ_2 is P_2, then $u_{\rm ff1} = z_{13}(u_{\rm ff2} = z_{23})$;
Rule 4: If σ_1 is N_1 and σ_2 is N_2, then $u_{\rm ff1} = z_{14}(u_{\rm ff2} = z_{24})$.

A. Responses to Sudden Load Disturbance

For testing the robustness of the proposed control method, conventional PD control method, and FLC method [17] against system uncertainties and load disturbances, the values of the output filter parameters are changed and the load disturbance is suddenly applied, i.e., no load to full load. It is well-known that the filter parameters may be affected by parasite resistance, temperature, their nonlinear characteristics, etc. In this paper, we assume that the uncertain values (ΔL_f and ΔC_f) of the filter parameters are $+60\%$ variations of their nominal values (i.e., $\Delta L_f = +0.6L_f$ and $\Delta C_f = +0.6C_f$) to certainly confirm the robustness to system uncertainties.

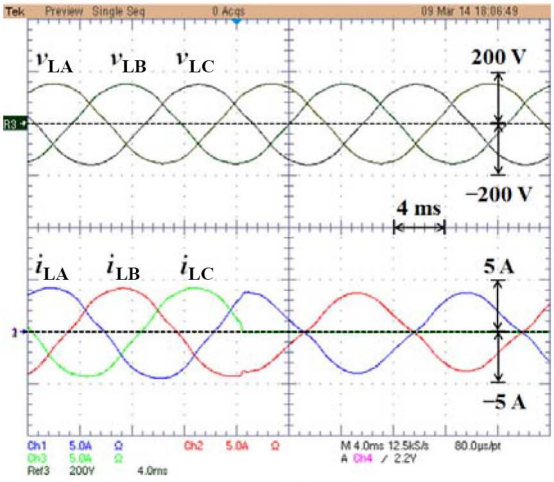

(a)

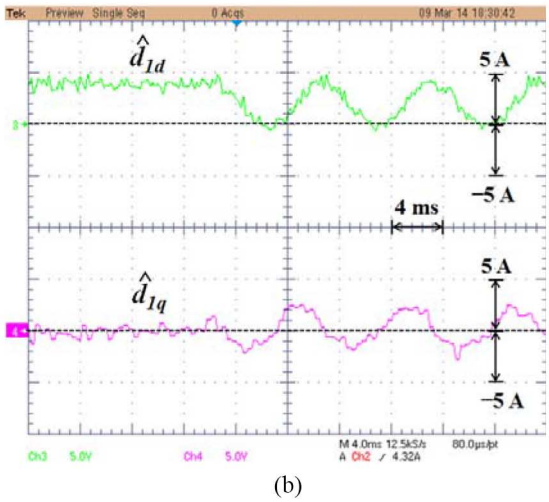

(b)

Fig. 9. Experimental results of the proposed control scheme under unbalanced load disturbance with system uncertainties ($\Delta L_f = +0.3L_f, \Delta C_f = +0.3C_f$). (a) Load voltages ($v_{\rm LA}, v_{\rm LB}, v_{\rm LC}$) and load currents ($i_{\rm LA}$, $i_{\rm LB}, i_{\rm LC}$). (b) Estimated disturbance ($\hat{d}_{1d}$, $\hat{d}_{1q}$).

Figs. 6−8 show the experimental results about the dynamic responses of the proposed method, conventional PD method, and FLC method under system parameters uncertainties when the load is suddenly changed from no load to full load, respectively. Each figure shows the waveforms of the load voltages ($v_{\rm LA}, v_{\rm LB}, v_{\rm LC}$), load currents ($i_{\rm LA}, i_{\rm LB}, i_{\rm LC}$), and load $d-q$ axis voltages (v_{Ld}, v_{Lq}). In addition, in Fig. 6(b), the estimated disturbance values ($\hat{d}_{1d}$, $\hat{d}_{1q}$) are presented to clarify the performance of the proposed disturbance observer. It is easy to see that the load voltage of the proposed controller in Fig. 6 is recovered to the steady-state much faster than those of the conventional PD control scheme and FLC scheme in Figs. 7 and 8 (i.e., voltage dip: 28/49/50 V, recovering time: 0.6/1/1 ms, respectively). From Figs. 6−8, it can be clearly observed that the load voltage of the proposed method has lower THD and smaller steady-state rms error in comparison with those of the conventional PD method and FLC method (THD: 0.34%/0.74%/0.75%, steady-state rms error: 0.2/1.6/1.1 V).

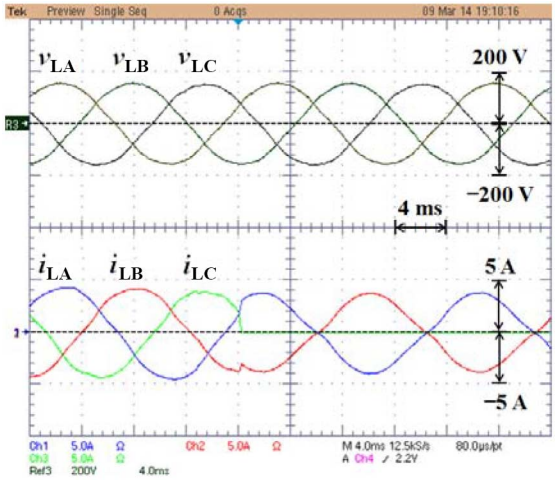

Fig. 10. Experimental results of the conventional PD control scheme under unbalanced load disturbance with system uncertainties ($\Delta L_f = +0.3L_f, \Delta C_f = +0.3C_f$): Load voltages ($v_{\rm LA}, v_{\rm LB}, v_{\rm LC}$) and load currents ($i_{\rm LA}, i_{\rm LB}, i_{\rm LC}$).

B. Responses to Unbalanced Load Disturbance

To further evaluate the robustness of three control methods against system uncertainties and load disturbances, the changes of the output filter parameters ($\Delta L_f = +0.3L_f$ and $\Delta C_f = +0.3C_f$) and the unbalanced load disturbance (i.e., only phase C is suddenly opened) are taken into account.

Figs. 9 and 10 show the experimental results of the proposed control system and conventional PD control system when the phase C is suddenly opened. It can be noticed that like in Figs. 6(b) and 9(b) only includes the estimated disturbances ($\hat{d}_{1d}$, $\hat{d}_{1q}$) because it is not easy to obtain the disturbance values (d_{1d}, d_{1q}) in experiments. It is observed from Figs. 9 and 10 that the load output voltages of the proposed method are controlled well in spite of the system parameter uncertainties ($\Delta L_f = +0.3L_f$ and $\Delta C_f = +0.3C_f$) and the suddenly opened phase C, i.e., the THDs and steady-state rms error of the load voltage are about 0.38% and 0.2 V for the proposed method in Fig. 9 and about 0.85% and 1.6 V for the conventional PD method in Fig. 10.

C. Responses to Nonlinear Load

In order to assess the voltage regulation performance of three control methods, a three-phase full-bridge diode rectifier, which is connected to an RLC load on the dc side (i.e., $R_n = 65\ \Omega$, $L_n = 15\,\text{mH}$, and $C_n = 220\,\mu\text{F}$), is utilized as a nonlinear load as seen in Fig. 3(a). In this case, the system parameter uncertainties ($\Delta L_f = +0.3L_f$ and $\Delta C_f = +0.3C_f$) are also considered to demonstrate the robustness of three control schemes.

Figs. 11 and 12 illustrate the experimental results of the proposed control method and conventional PD control method under nonlinear load, respectively. It is seen that the steady-state response of the proposed scheme achieves lower THD (1.05%) compared to that of the conventional PD scheme (2.43%). Furthermore, the steady-state error of the proposed

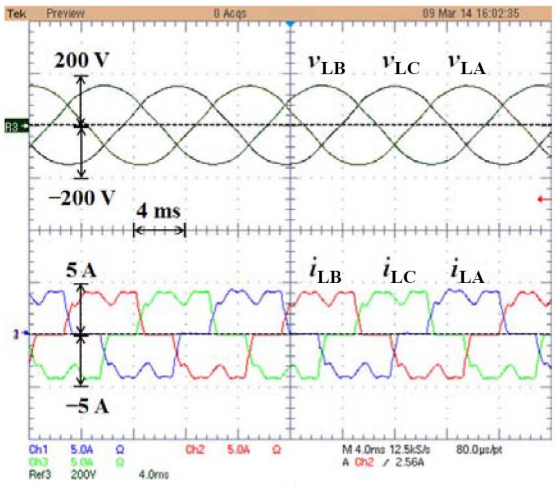

(a)

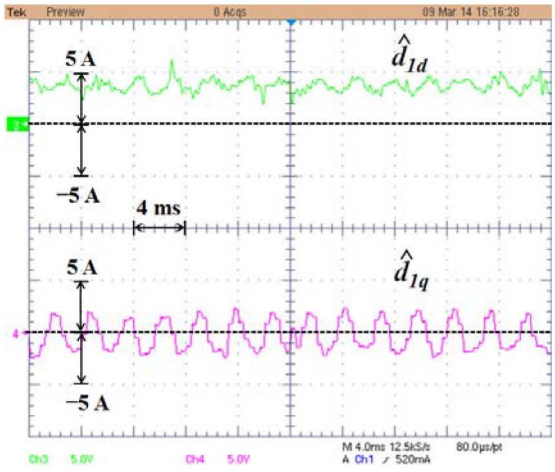

(b)

Fig. 11. Experimental results of the proposed control scheme under nonlinear load with system uncertainties ($\Delta L_f = +0.3L_f, \Delta C_f = +0.3C_f$). (a) Load voltages ($v_{\rm LA}, v_{\rm LB}, v_{\rm LC}$) and load currents ($i_{\rm LA}, i_{\rm LB}, i_{\rm LC}$). (b) Estimated disturbance ($\hat{d}_{1d}$, $\hat{d}_{1q}$).

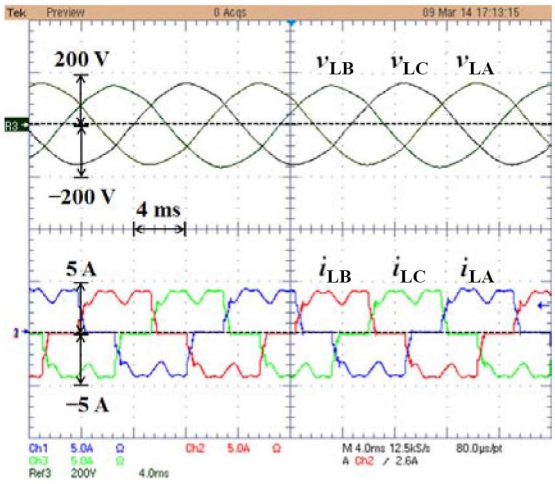

Fig. 12. Experimental results of the conventional PD control scheme under nonlinear load with system uncertainties ($\Delta L_f = +0.3L_f, \Delta C_f = +0.3C_f$): Load voltages ($v_{\rm LA}, v_{\rm LB}, v_{\rm LC}$) and load currents ($i_{\rm LA}, i_{\rm LB}, i_{\rm LC}$).

TABLE II
PERFORMANCE SUMMARY OF THREE CONTROL METHODS

Case	Criteria	Proposed method	Conventional PD method	FLC method [17]
Sudden load	Dip voltage (V)	28	49	50
	THD (%)	0.34	0.74	0.75
	RMS (V)	109.8	108.4	108.9
Unbalanced load	THD (%)	0.38	0.85	0.87
	RMS (V)	109.8	108.4	108.8
Nonlinear load	THD (%)	1.05	2.43	2.31
	RMS (V)	109.7	108.3	108.7

method (0.3 V) is smaller than that of the conventional PD method (1.7 V).

Note that the experimental waveforms of the FLC method are shown only under sudden load disturbance with system uncertainties because of the limited space. However, Table II provides the performance comparison (i.e., dip voltage in transient-state, rms value, and THD) of three control strategies about three cases during the transient and steady-state based on the experimental results.

V. CONCLUSION

In this paper, a disturbance observer-based fuzzy adaptive voltage control strategy was presented for a single standalone DG unit. Also, the transient response of the proposed controller is quite fast since the output voltage is directly controlled using only a voltage control loop. By proposing a disturbance observer and including it in the control system, the proposed control strategy is robust to system uncertainties. Experimental results demonstrated the better transient and steady-state performances of the proposed control scheme under various load conditions (i.e., sudden load disturbances, system parameter uncertainties, and nonlinear load) in comparison with the conventional PD control method and the FLC method.

REFERENCES

[1] A. Bidram, A. Davoudi, and F. L. Lewis, "A multiobjective distributed control framework for islanded AC microgrids," *IEEE Trans. Ind. Informat.*, vol. 10, no. 3, pp. 1785–1798, Aug. 2014.
[2] R. Pena-Alzola *et al.*, "Systematic design of the lead-lag network method for active damping in LCL-filter based three phase converters," *IEEE Trans. Ind. Informat.*, vol. 10, no. 1, pp. 43–52, Feb. 2014.
[3] Q. Shafiee, J. M. Guerrero, and J. C. Vasquez, "Distributed secondary control for islanded microgrids-a novel approach," *IEEE Trans. Power Electron.*, vol. 29, no. 2, pp. 1018–1031, Feb. 2014.
[4] H. L. Ginn and G. Chen, "Digital control method for grid-connected converters supplied with nonideal voltage," *IEEE Trans. Ind. Informat.*, vol. 10, no. 1, pp. 127–136, Feb. 2014.
[5] J. Yin, S. Duan, and B. Liu, "Stability analysis of grid-connected inverter with LCL filter adopting a digital single-loop controller with inherent damping characteristic," *IEEE Trans. Ind. Informat.*, vol. 9, no. 2, pp. 1104–1112, May 2013.
[6] V. Yaramasu, M. Rivera, B. Wu, and J. Rodriguez, "Model predictive current control of two-level four-leg inverters-part I: Concept, algorithm, and simulation analysis," *IEEE Trans. Power Electron.*, vol. 28, no. 7, pp. 3459–3468, Jul. 2013.
[7] J. R. Fischer, S. A. Gonzalez, M. A. Herran, M. G. Judewicz, and D. O. Carrica, "Calculation-delay tolerant predictive current controller for three-phase inverters," *IEEE Trans. Ind. Informat.*, vol. 10, no. 1, pp. 233–242, Feb. 2014.

[8] C. Xia, T. Liu, T. Shi, and Z. Song, "A simplified finite-control-set model-predictive control for power converters," *IEEE Trans. Ind. Informat.*, vol. 10, no. 2, pp. 991–1002, May 2014.
[9] M. Hua, H. Hu, Y. Xing, and J. M. Guerrero, "Multilayer control for inverters in parallel operation without intercommunications," *IEEE Trans. Power Electron.*, vol. 27, no. 8, pp. 3651–3663, Aug. 2012.
[10] Q. C. Zhong, "Robust droop controller for accurate proportional load sharing among inverters operated in parallel," *IEEE Trans. Ind. Electron.*, vol. 60, no. 4, pp. 1281–1290, Apr. 2013.
[11] T. B. Lazzarin and I. Barbi, "DSP-based control for parallelism of three-phase voltage source inverter," *IEEE Trans. Ind. Informat.*, vol. 9, no. 2, pp. 749–759, May 2013.
[12] P. Cortes *et al.*, "Model predictive control of an inverter with output LC filter for UPS applications," *IEEE Trans. Ind. Electron.*, vol. 56, no. 6, pp. 1875–1883, Jun. 2009.
[13] R. O. Ramirez *et al.*, "Predictive controller for a three-phase/single-phase voltage source converter cell," *IEEE Trans. Ind. Informat.*, vol. 10, no. 3, pp. 1878–1889, Aug. 2014.
[14] S. Jiang, D. Cao, Y. Li, J. Liu, and F. Z. Peng, "Low-THD, fast-transient, and cost-effective synchronous-frame repetitive controller for three-phase UPS inverters," *IEEE Trans. Power Electron.*, vol. 27, no. 6, pp. 2994–3005, Jun. 2012.
[15] G. Escobar, A. A. Valdez, J. Leyva-Ramos, and P. Mattavelli, "Repetitive-based controller for a UPS inverter to compensate unbalance and harmonic distortion," *IEEE Trans. Ind. Electron.*, vol. 54, no. 1, pp. 504–510, Feb. 2007.
[16] H. Deng, R. Oruganti, and D. Srinivasan, "Analysis and design of iterative learning control strategies for UPS inverters," *IEEE Trans. Ind. Electron.*, vol. 54, no. 3, pp. 1739–1751, Jun. 2007.
[17] D. E. Kim and D. C. Lee, "Feedback linearization control of three-phase UPS inverter systems," *IEEE Trans. Ind. Electron.*, vol. 57, no. 3, pp. 963–968, Mar. 2010.
[18] A. Houari, H. Renaudineau, J. P. Pierfederici, and F. Meibody-Tabar, "Flatness-based control of three-phase inverter with output LC filter," *IEEE Trans. Ind. Electron.*, vol. 59, no. 7, pp. 2890–2897, Jul. 2012.
[19] T. L. Tai and J. S. Chen, "UPS inverter design using discrete-time sliding-mode control scheme," *IEEE Trans. Ind. Electron.*, vol. 49, no. 1, pp. 67–75, Feb. 2002.
[20] H. Komurcugil, "Rotating-sliding-line-based sliding-mode control for single-phase UPS inverters," *IEEE Trans. Ind. Electron.*, vol. 59, no. 10, pp. 3719–3726, Oct. 2012.
[21] H. Karimi, E. J. Davision, and R. Iravani, "Multivariable servomechanism controller for autonomous operation of a distributed generation unit: design and performance evaluation," *IEEE Trans. Power Syst.*, vol. 25, no. 2, pp. 853–865, May 2010.
[22] M. Dai, M. N. Marwali, J. W. Jung, and A. Keyhani, "A three-phase four-wire inverter control technique for a single distributed generation unit in island mode," *IEEE Trans. Power Electron.*, vol. 23, no. 1, pp. 322–331, Jan. 2008.
[23] P. Mattavelli, G. Escobar, and A. M. Stankovic, "Dissipativity-based adaptive and robust control of UPS," *IEEE Trans. Ind. Electron.*, vol. 48, no. 2, pp. 334–343, Apr. 2001.
[24] G. E. Valderrama, A. M. Stankovic, and P. Mattavelli, "Dissipativity-based adaptive and robust control of UPS in unbalanced operation," *IEEE Trans. Power Electron.*, vol. 18, no. 4, pp. 1056–1062, Jul. 2003.
[25] T. D. Do, V. Q. Leu, Y. S. Choi, H. H. Choi, and J. W. Jung, "An adaptive voltage control strategy of three-phase inverter for standalone distributed generation systems," *IEEE Trans. Ind. Electron.*, vol. 60, no. 12, pp. 5660–5672, Dec. 2013.
[26] J. W. Jung *et al.*, "Three-phase inverter for a standalone distributed generation system: adaptive voltage control design and stability analysis," *IEEE Trans. Energy Convers.*, vol. 29, no. 1, pp. 46–56, Mar. 2014.
[27] T. Hirose and H. Matsuo, "Standalone hybrid wind-solar power generation system applying dump power control without dump load," *IEEE Trans. Ind. Electron.*, vol. 59, no. 2, pp. 988–997, Feb. 2012.
[28] P. Thounthong *et al.*, "DC bus stabilization of Li-ion battery based energy storage for a hydrogen/solar power plant for autonomous network applications," *IEEE Trans. Ind. Appl.*, in press.
[29] Z. Zhang, Y. Cai, Y. Zhang, D. Gu, and Y. Liu, "A distributed architecture based on micro-bank modules with self-reconfiguration control to improve the energy efficiency in the battery energy storage system," *IEEE Trans. Power Electron.*, in press.
[30] N. A. Orlando, M. Liserre, R. A. Mastromauro, and A. Dell'Aquila, "A survey of control issues in PMSG-based small wind-turbine systems," *IEEE Trans. Ind. Informat.*, vol. 9, no. 3, pp. 1211–1221, Aug. 2013.
[31] L. X. Wang, "Stable adaptive fuzzy control of nonlinear systems," *IEEE Trans. Fuzzy Syst.*, vol. 1, no. 2, pp. 146–155, May 1993.
[32] F. L. Lewis, C. T. Abdallah, and D. M. Dawson, *Control of Robot Manipulators*. New York, NY, USA: MacMillan, 1993.
[33] S. H. Zak, *Systems and Control*. London, U.K.: Oxford Univ. Press, 2003.
[34] J. W. Jung, Y. S. Choi, V. Q. Leu, and H. H. Choi, "Fuzzy PI-type current controllers for permanent magnet synchronous motors," *IET Elect. Power Appl.*, vol. 5, no. 1, pp. 143–152, Jan. 2011.

Dong Quang Dang received the B.S. and M.S. degrees in electrical engineering from the Hanoi University of Science and Technology, Hanoi, Vietnam, in 2005 and 2010, respectively, and the Ph.D. degree in electrical engineering from Dongguk University, Seoul, Korea, in 2015.

From 2006 to 2011, he worked as a Lecturer with the Hung Yen University of Technology and Education, Hung Yen, Vietnam. His research interests include electric machine drives and control of distributed generation systems using renewable energy sources.

Young-Sik Choi received the B.S. degree in electrical engineering from Dongguk University, Seoul, Korea, in 2009. He is currently pursuing the Ph.D. degree in electronics and electrical engineering at the same university.

His research interests include electric machine drives based on microprocessor and control of distributed generation systems using renewable energy sources.

Han Ho Choi (M'03) received the B.S. degree in control and instrumentation engineering from Seoul National University, Seoul, Korea, in 1988, and the M.S. and Ph.D. degrees in electrical engineering from the Korea Advanced Institute of Science and Technology, Daejeon, Korea, in 1990 and 1994, respectively.

He is currently with the Division of Electronics and Electrical Engineering, Dongguk University, Seoul. His research interests include control theory and its application to real world problems.

Jin-Woo Jung (S'97–M'06) received the B.S. and M.S. degrees in electrical engineering from Hanyang University, Seoul, Korea, in 1991 and 1997, respectively, and the Ph.D. degree in electrical and computer engineering from Ohio State University, Columbus, OH, USA, in 2005.

From 1997 to 2000, he was with the Digital Appliance Research Laboratory, LG Electronics Co., Ltd., Seoul. From 2005 to 2008, he was a Senior Engineer with the R&D Center and with the Plasma Display Panel Development Team, Samsung SDI Co., Ltd., Yongin, Korea. Since 2008, he has been an Associate Professor with the Division of Electronics and Electrical Engineering, Dongguk University, Seoul. His research interests include digital-signal-processor-based electric machine drives, distributed generation systems using renewable energy sources, and power conversion systems and drives for electric vehicles.